EPFL
École polytechnique fédérale de Lausanne

Institute of Materials - Institute of Bioengineering
sunmil.epfl.ch

SuNMiL
Supramolecular NanoMaterials and Interfaces Laboratory

Coherent and Semi-coherent Grain Boundaries
Lesson 10

MSE 304

Francesco Stellacci

桑缪 썬밀 सानमिल ΣouNMιΛ سنمل CaHMПЛ

Reading for this Class

Homophase Grain Boundaries

Key Topics in the Previous Class

Coincidence Lattice Description of a Generic Grain Boundaries

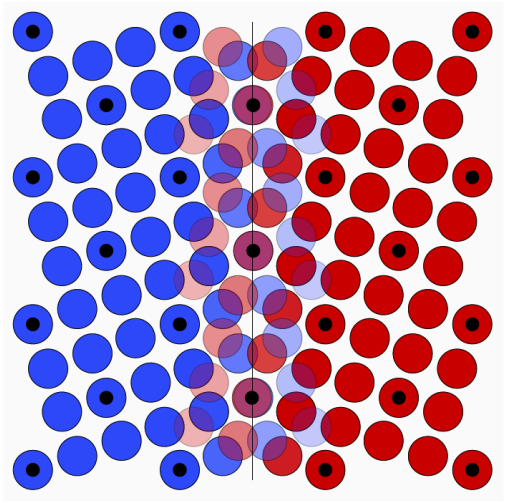

sc, $\mathbf{n} = (100)$,
$\mathbf{u} = \langle 001 \rangle$, $\theta = 36.9°$

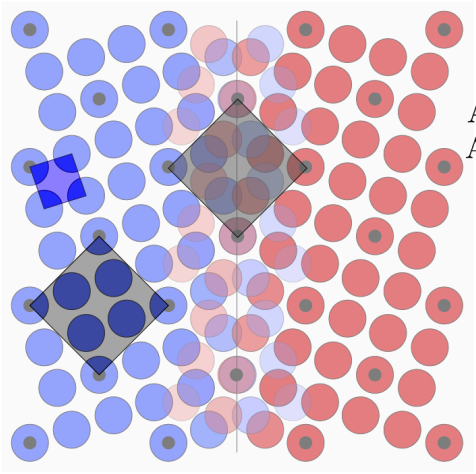

Atoms per unit cell: 1
Atoms per CSL cell: 5

$\boxed{\Sigma = 5}$

sc, $\mathbf{n} = (100)$,
$\mathbf{u} = \langle 001 \rangle$, $\theta = 36.9°$

Coincidence Lattice Description of a Generic Grain Boundaries

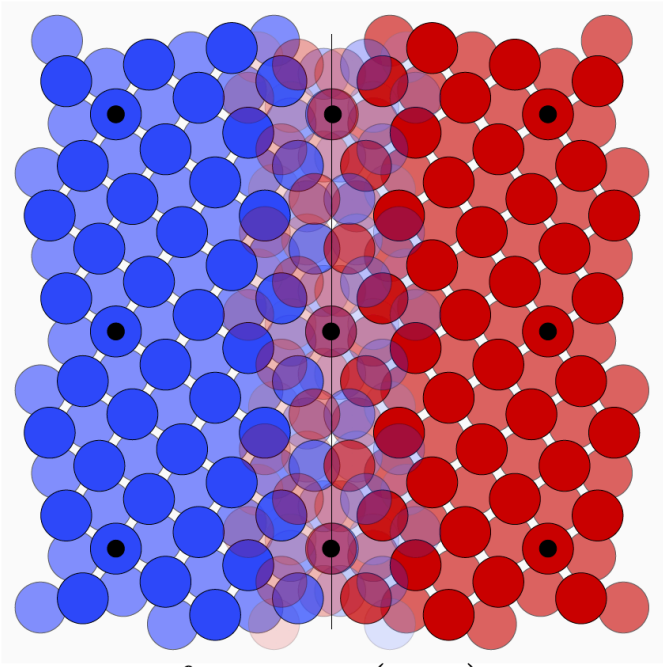

fcc, $\mathbf{n} = (100)$,
$\mathbf{u} = \langle 001 \rangle$, $\theta = 22.6°$
$\boxed{\Sigma = 13a}$

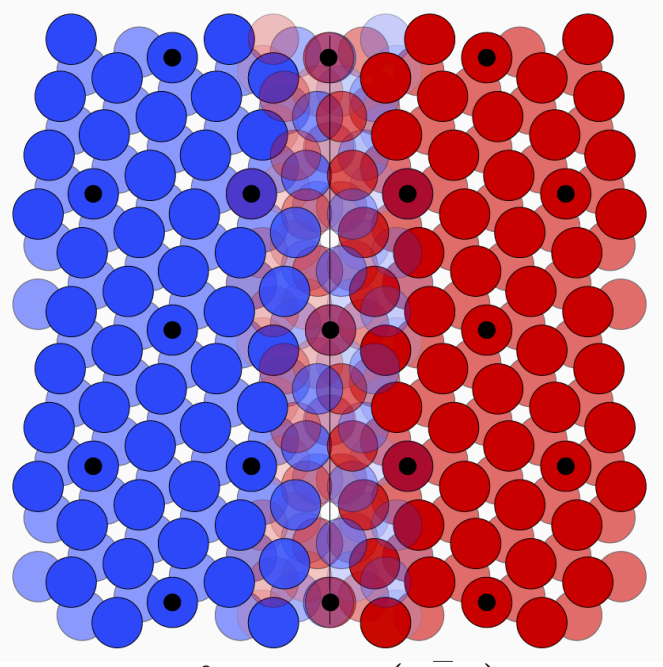

fcc, $\mathbf{n} = (1\bar{1}0)$,
$\mathbf{u} = \langle 111 \rangle$, $\theta = 38.21°$
$\boxed{\Sigma = 7}$

CSL Selection Rules

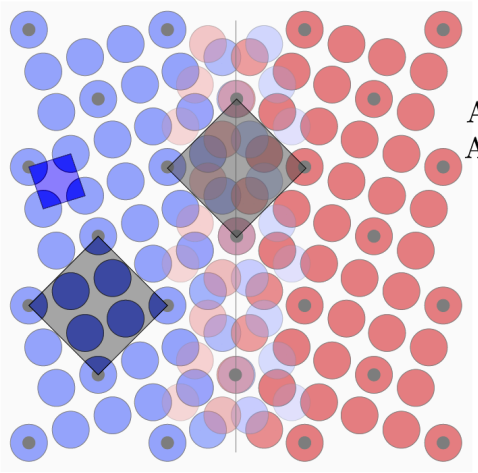

Atoms per unit cell: 1
Atoms per CSL cell: 5

$\boxed{\Sigma = 5}$

sc, $\mathbf{n} = (100)$,
$\mathbf{u} = \langle 001 \rangle$, $\theta = 36.9°$

$$\Sigma = x^2 + Ny^2$$

$$N = u^2 + v^2 + w^2$$

$$\theta = \tan^{-1}\left(\frac{y}{x}\right) N^{\frac{1}{2}}$$

Displacement Shift Complete Lattice

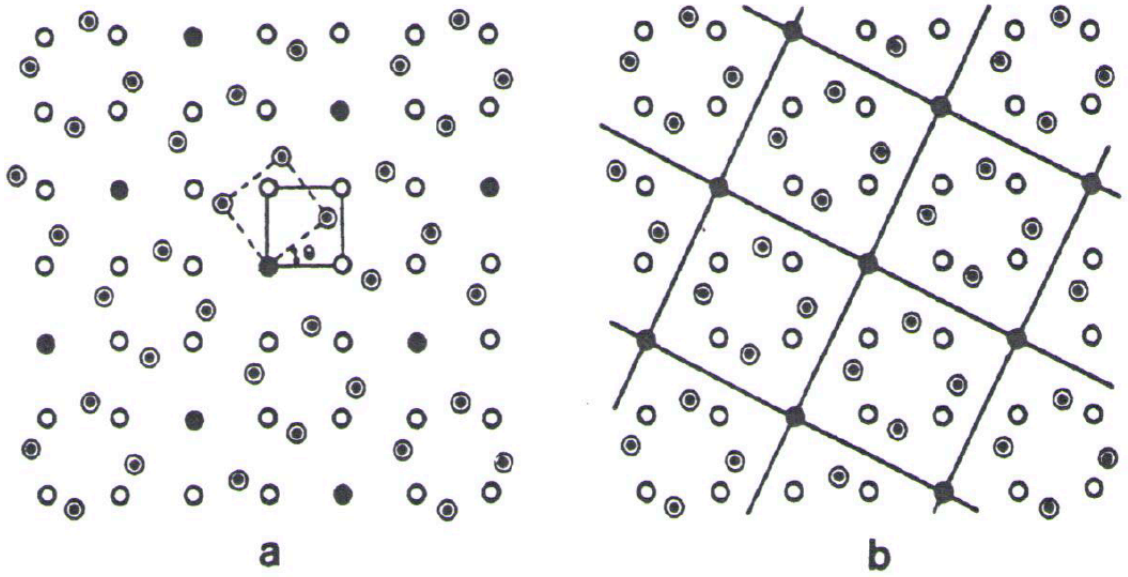

Displacement Shift Complete Lattice

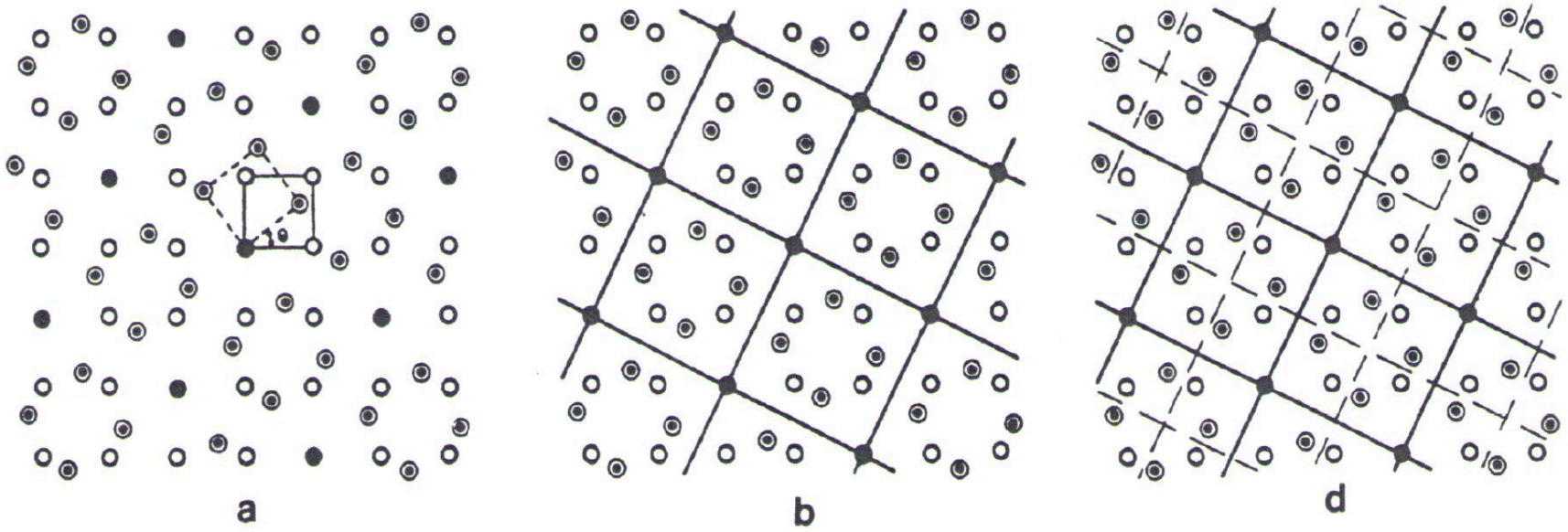

Displacement Shift Complete Lattice

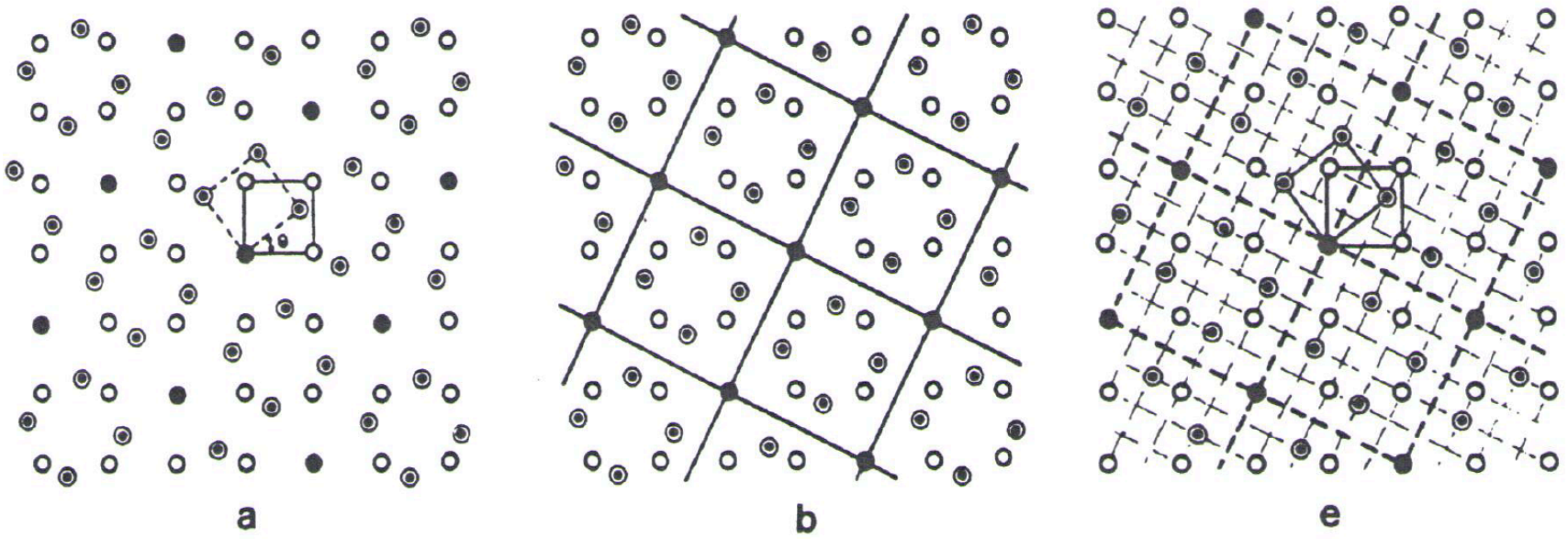

Displacement Shift Complete Lattice

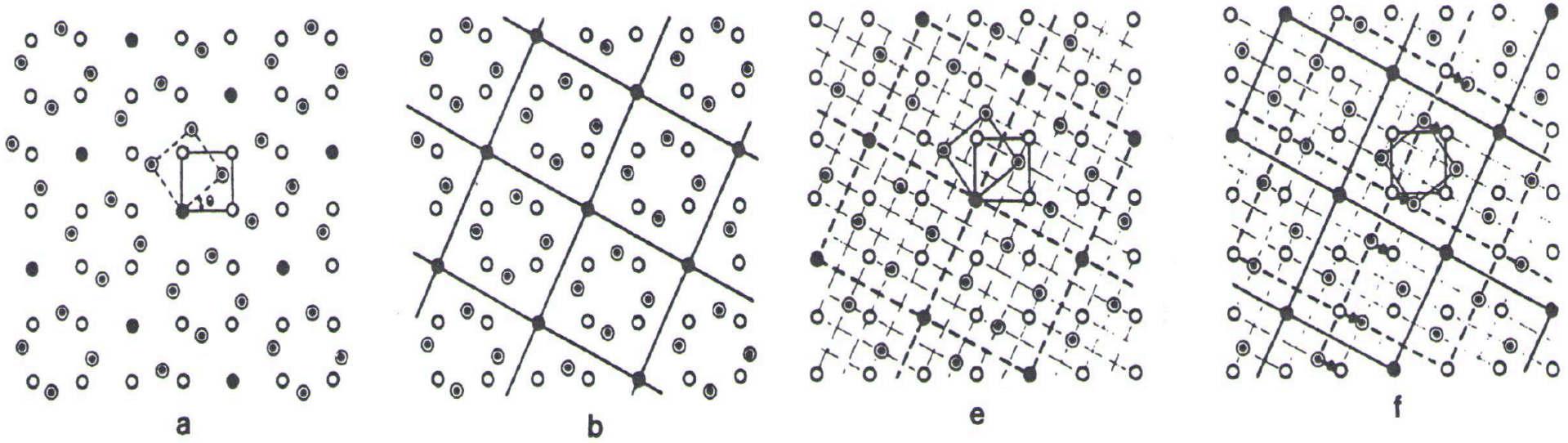

Displacement Shift Complete Lattice

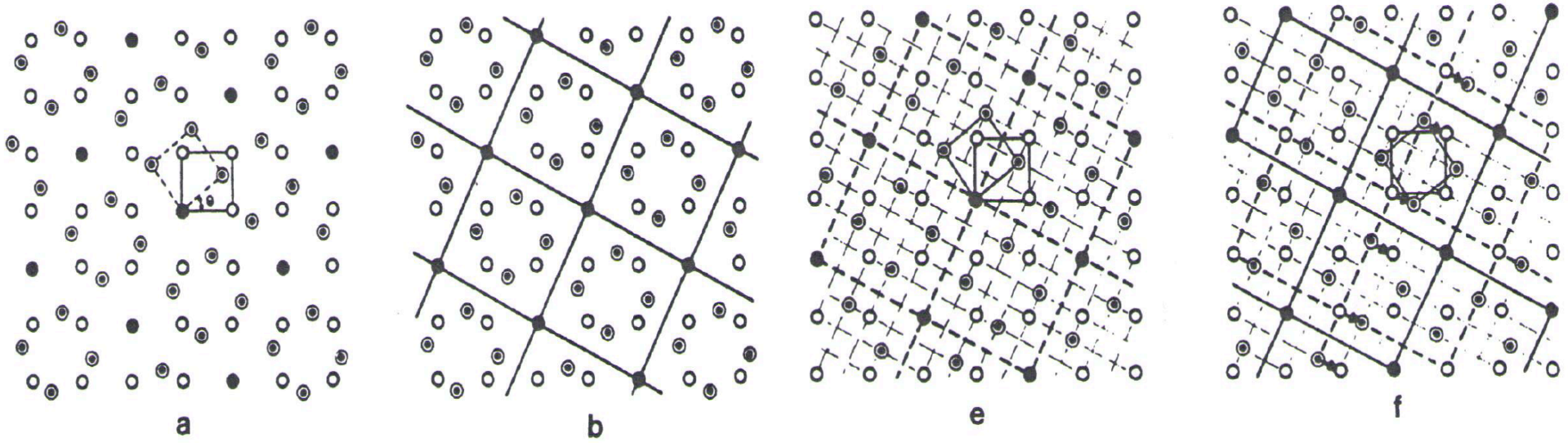

Defects at a Coherent Homophase Interfase (CHI)

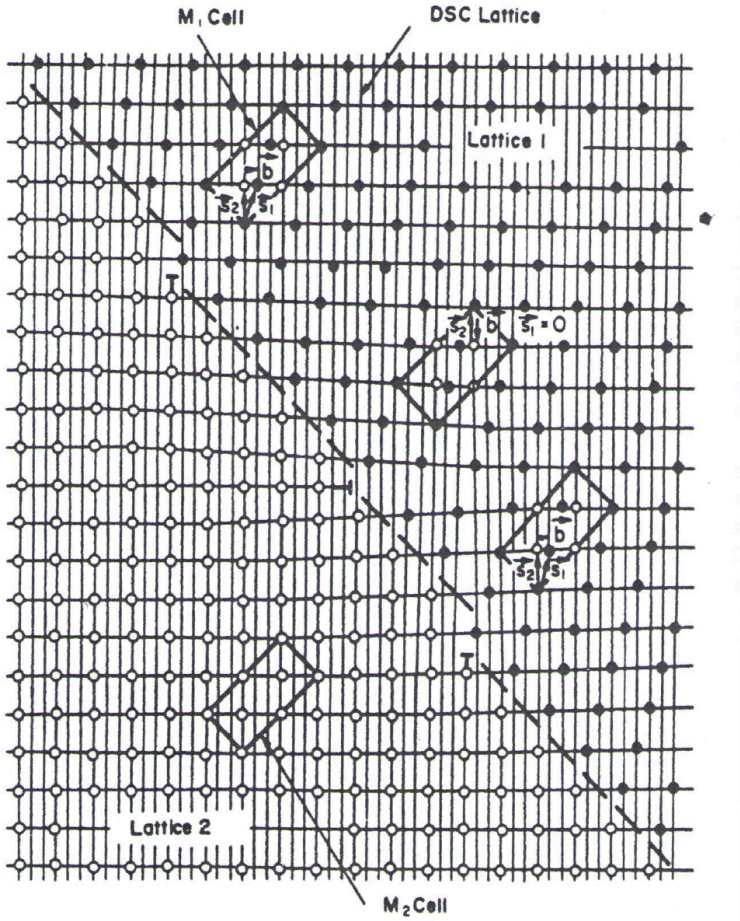

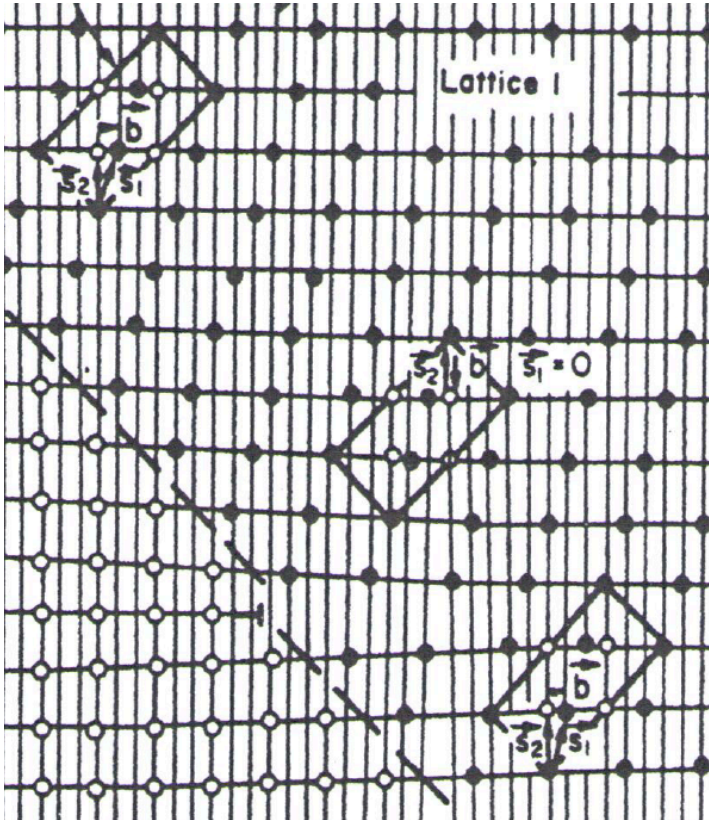

Ledges and Grain Boundaries

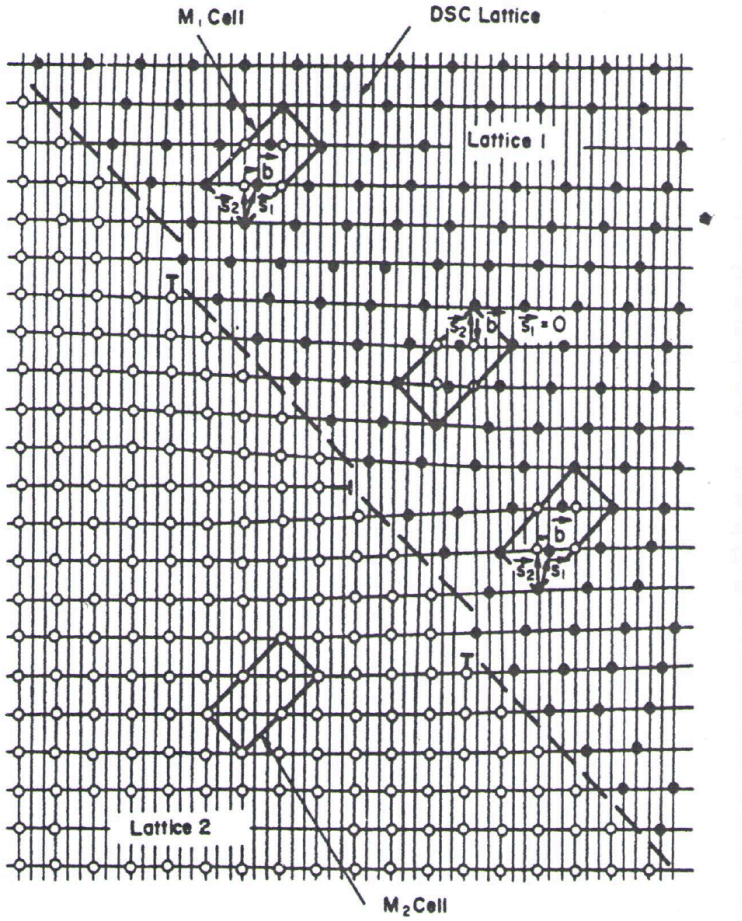

Misfit Dislocation in CHI

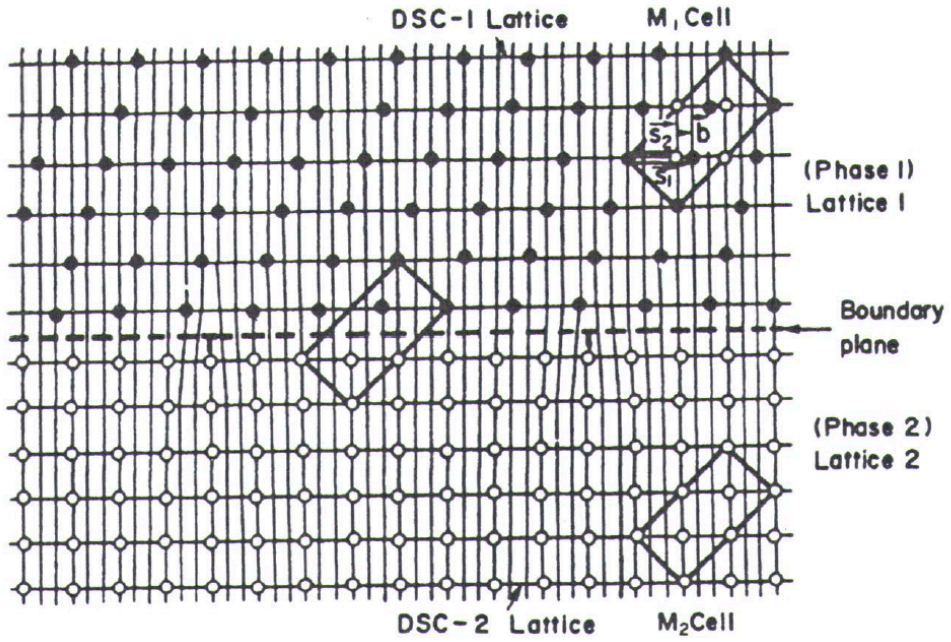

Figure 13.24. The interphase boundary between two different lattices (phases) M_1 and M_2, which form a planar interface containing interfacial dislocations with a spacing determined by O-lattice theory. The Burgers vector and ledge vectors of the interfacial dislocations are shown in the diagram in the upper right. The DSC lattice is indicated by fine lines in the figure. Reprinted with permission from [53] by Elsevier Science Ltd., Oxford, England.

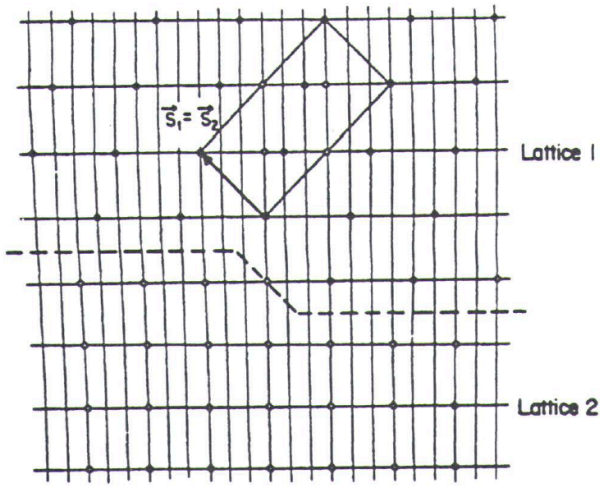

Figure 13.26. Pure ledge in the interphase boundary illustrated previously in Figure 13.24. The ledge vectors are shown above the ledge. Reprinted with permission from [53] by Elsevier Science Ltd., Oxford, England.

SuNMIL EPFL

Misfit Dislocations in Semi-coherent Interfaces

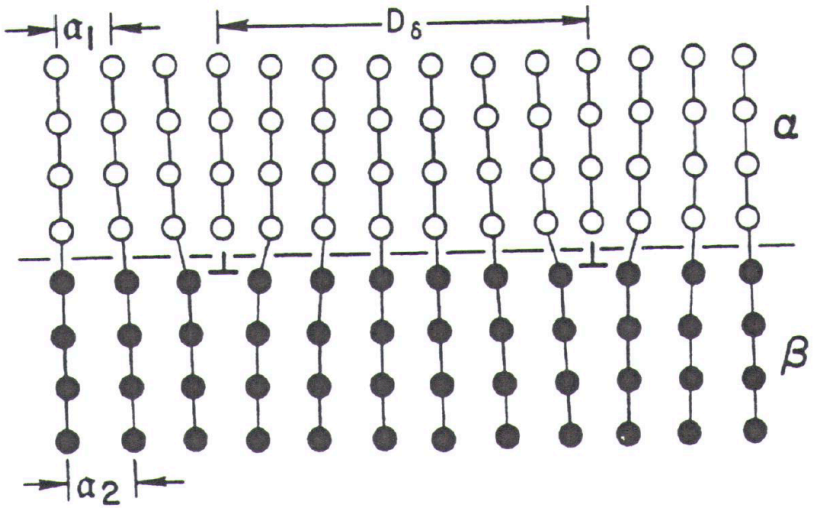

Misfit Dislocations in Semi-coherent Interfaces

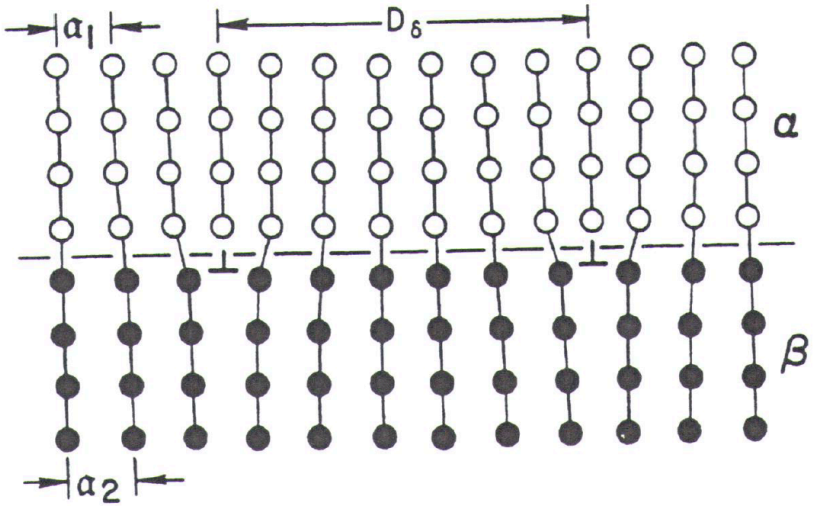

$$D_\delta = na_1 = (n+1)a_2 \qquad n = \frac{a_2}{a_1 - a_2}$$

$$a' = \frac{a_1 + a_2}{2}$$

$$D_\delta = \left(n + \frac{1}{2}\right) a'$$

$$D_\delta = \frac{(a_1 + a_2)^2}{4(a_1 - a_2)}$$

$$\delta = \frac{2(a_1 - a_2)}{a_1 + a_2} = \frac{a_1 - a_2}{a'}$$

$$D_\delta = \frac{a'}{\delta} = \frac{b}{\delta}$$

Twin Boundaries

- Close-packed *fcc* have very low-energy **twin** grain boundaries, that correspond to reversal of the ABCABC stacking order

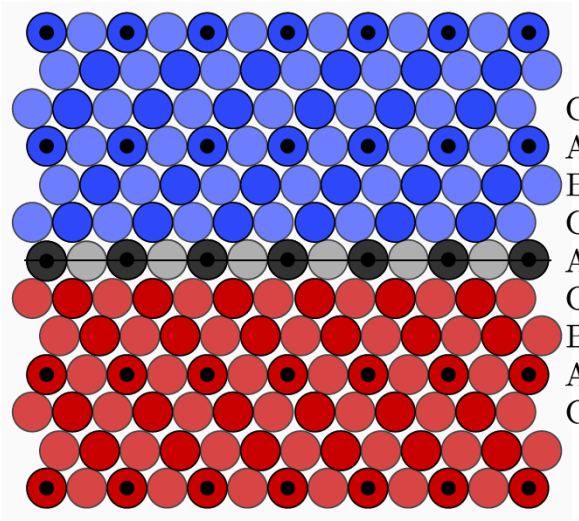

fcc,
$\mathbf{n} = (111)\ \psi = 180°$
$\boxed{\Sigma = 3}$

Stacking Faults

- Twins are closely related to **stacking faults**, ABCBCAB or ABCBABC

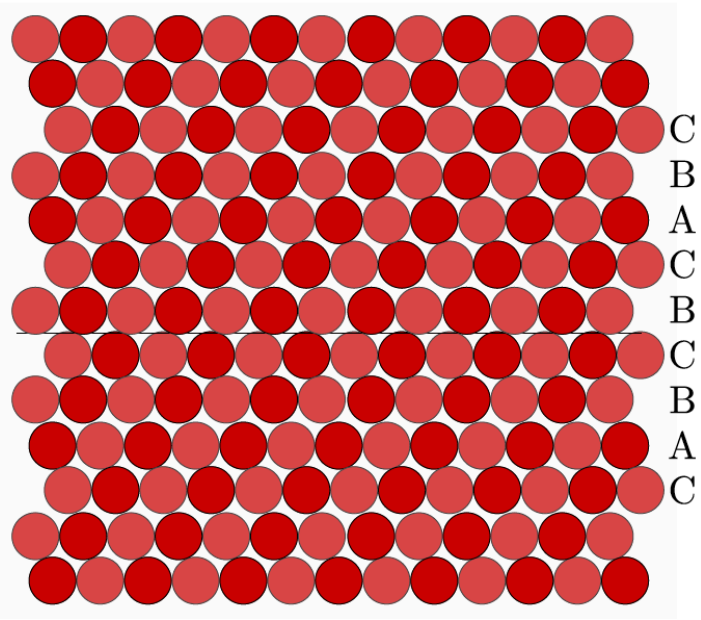

fcc,
$\mathbf{n} = (111)$

Stacking Faults and Twin Boundaries

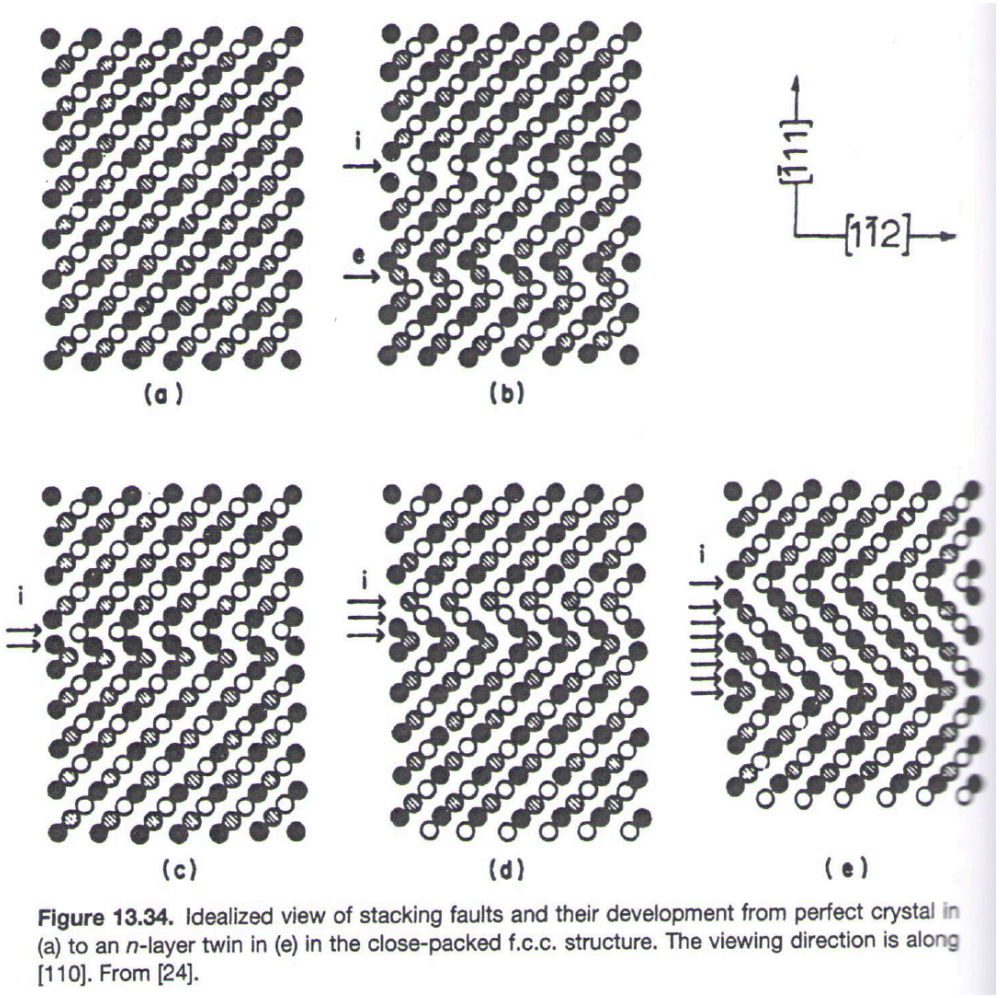

Figure 13.34. Idealized view of stacking faults and their development from perfect crystal in (a) to an *n*-layer twin in (e) in the close-packed f.c.c. structure. The viewing direction is along [110]. From [24].

Stacking Faults

- Twins are closely related to **stacking faults**, ABCBCAB or ABCBABC
  - Stacking faults can be thought as a pair of twins, and in fact $\gamma_{sf} \approx 2\gamma_t$

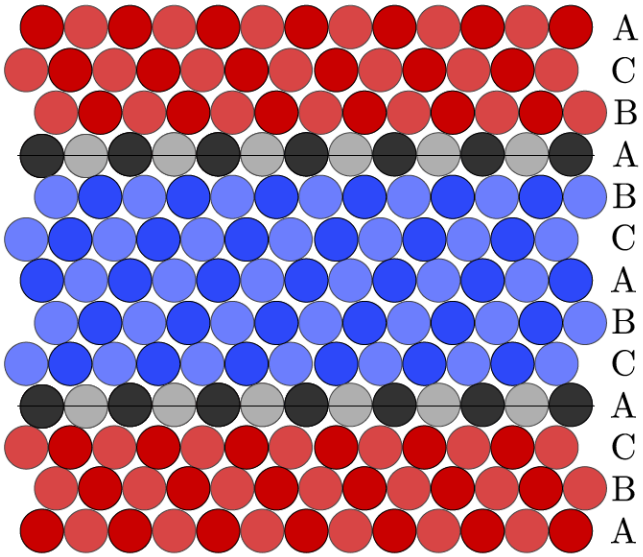

fcc,
$\mathbf{n} = (111)$

Stacking Faults and Twin Boundaries

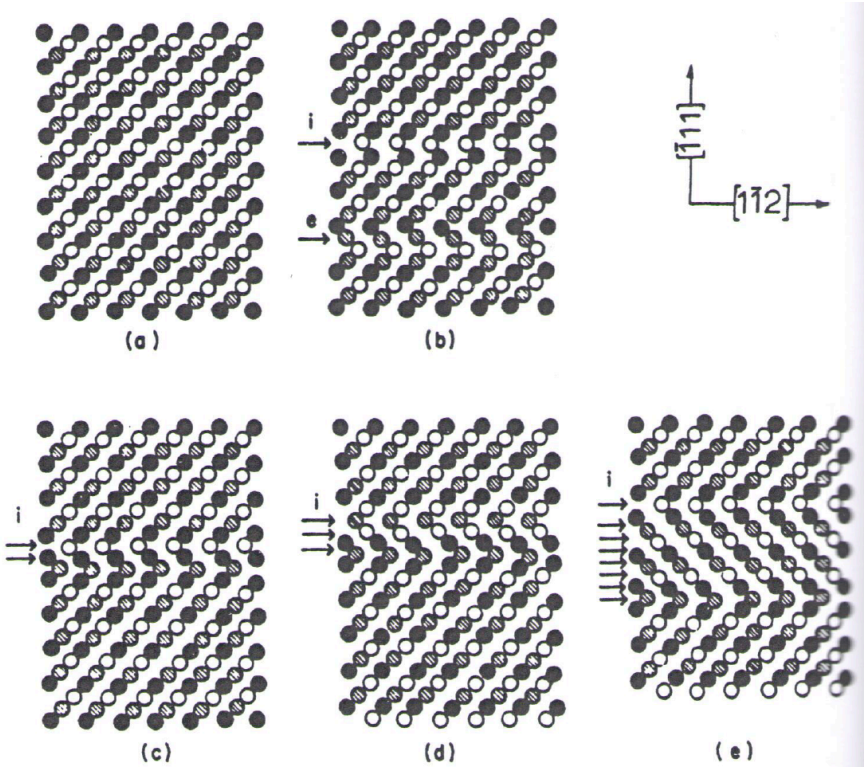

Figure 13.34. Idealized view of stacking faults and their development from perfect crystal in (a) to an *n*-layer twin in (e) in the close-packed f.c.c. structure. The viewing direction is along [110]. From [24].

$$\gamma_t = \Sigma\,[2n\phi_{3n} + n(\phi_{3n-1} + \phi_{3n+1})]$$
$$= \phi_2 + 2\phi_3 + \phi_4 + \ldots, \qquad (13.31)$$

$$\gamma_{esf} = \Sigma\,[2\phi_{3n-1} + (3n+1)\phi_{3n} + 3n\phi_{3n+1}]$$
$$= 2\phi_2 + 4\phi_3 + 3\phi_4 + \ldots, \qquad (13.32)$$

$$\gamma_{isf} = \Sigma\,[(3n-1)\phi_{3n-1} + 3n\phi_{3n}]$$
$$= 2\phi_2 + 3\phi_3 + 0\phi_4 + \ldots, \qquad (13.33)$$

$$\gamma_{hcp} = \Sigma\,[\Psi_{6n-2} + \Psi_{6n-3} + \Psi_{6n-4})]$$
$$= \phi_2 + \phi_3 + \phi_4 + \ldots. \qquad (13.34)$$

Roughening at Domain Boundaries

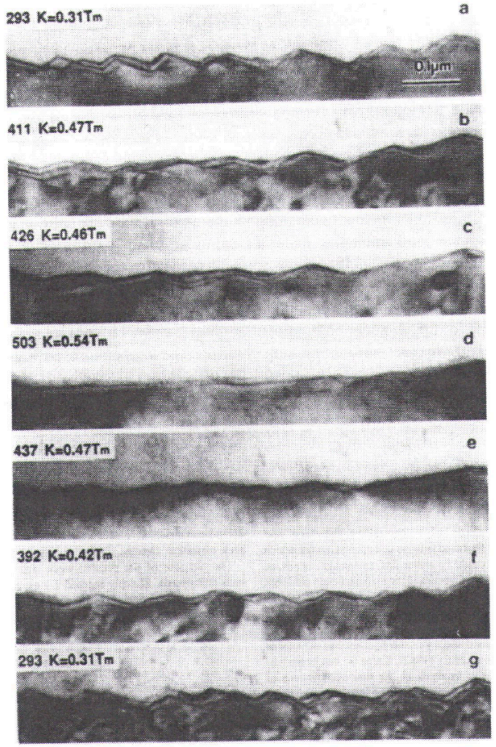

Figure 13.35. Reversible roughening–faceting transformation of an initially faceted $\Sigma = 3$ asymmetric <111> tilt boundary containing $\{112\}_1/\{112\}_2$ facets in aluminum as a function of step-wise heating (a-d) and subsequent cooling (d-g). Time at each temperature ≅ 30 min. Reprinted with permission from [75] by Elsevier Science Ltd., Oxford, England.

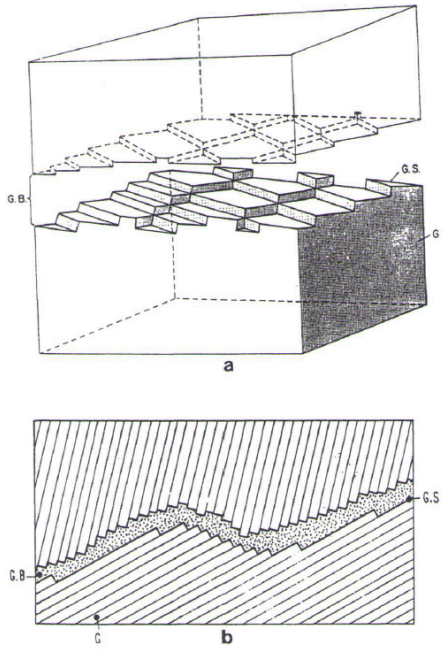

Figure 13.39. (a) Model of a migrating grain boundary. *GS* is the surface of both grains (*G*) with a ledge structure. The interspace between both grains forms the grain boundary (*GB*), which is assumed to be on the order of the ledge height. (b) Formation of large grain boundary ledges by the coagulation of monatomic ledges. Reprinted with permission from [83] by Elsevier Science Ltd., Oxford, England.

SuNMIL EPFL

Segregation at Domain Boundaries

- The type, stability, and mechanical properties of grain boundaries can be tuned by the presence of impurities
- Interstitial or substitutional impurities can segregate at grain boundaries because they can better accommodate lattice mismatch
- Gibbs absorption equation holds: $\frac{\partial \gamma}{\partial c} \approx -\Gamma / c$. Segregating atoms lower γ_{GB}

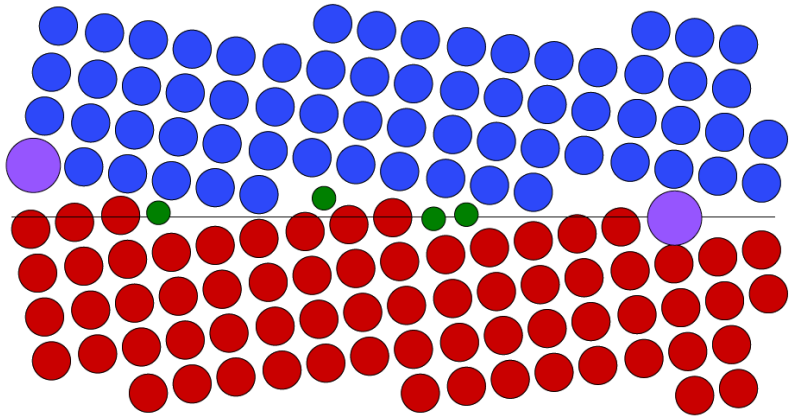

sc, $\mathbf{u} = \langle 001 \rangle$,
$\mathbf{n} = (100)$, $\theta = 18°$

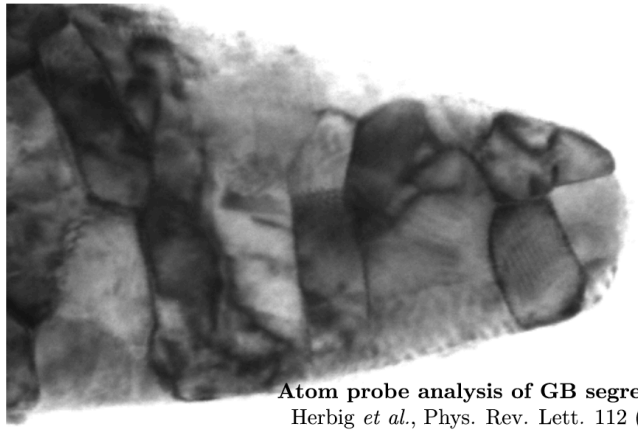

Atom probe analysis of GB segregation
Herbig *et al.*, Phys. Rev. Lett. 112 (2014)
Li *et al.*, Phys. Rev. Lett. 113 (2014)

Segregation at Domain Boundaries

- The type, stability, and mechanical properties of grain boundaries can be tuned by the presence of impurities
- Interstitial or substitutional impurities can segregate at grain boundaries because they can better accommodate lattice mismatch
- Gibbs absorption equation holds: $\frac{\partial \gamma}{\partial c} \approx -\Gamma / c$. Segregating atoms lower γ_{GB}

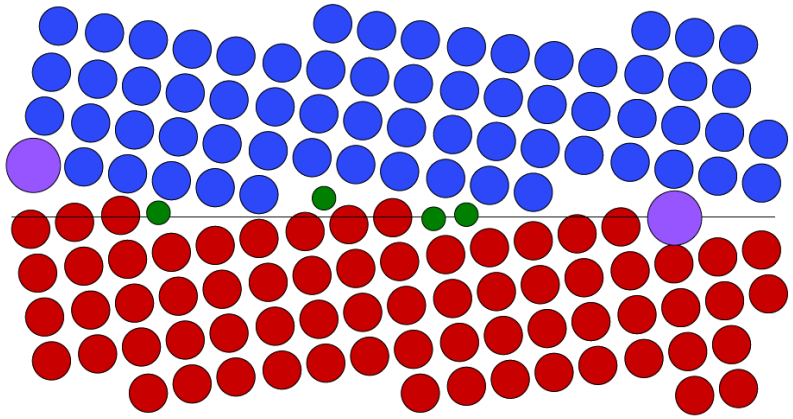

sc, $\mathbf{u} = \langle 001 \rangle$,
$\mathbf{n} = (100)$, $\theta = 18°$

$$\frac{X_{gb}}{1 - X_{gb}} = \frac{X_B}{X_B^{sat}} \exp \frac{-\Delta G'}{RT}, \qquad (13.40)$$

$$\beta_{gb} = \frac{1}{X_B^{sat}} \exp \frac{-\Delta G'}{RT}. \qquad (13.42)$$

Conclusions